Spatiotemporal modelling of correlated small-area outcomes: Analyzing the shared and type-specific patterns of crime and disorder

Abstract

This research applies a Bayesian multivariate modelling approach to analyze the spatiotemporal patterns of physical disorder, social disorder, property crime, and violent crime at the small-area scale. Despite crime and disorder exhibiting similar spatiotemporal patterns, as hypothesized by broken windows and collective efficacy theories, past studies often analyze a single outcome and overlook the correlation structures between multiple crime and disorder types. Accounting for five covariates, the best fitting model partitions the residual risk of each crime and disorder type into one spatial shared component, one temporal shared component, and type-specific spatial, temporal, and space-time components. The shared components capture the underlying spatial pattern and time trend common to all types of crime and disorder. Results show that population size, residential mobility, and the central business district are positively associated with all outcomes. The spatial shared component is found to explain the largest proportion of residual variability for all types of crime and disorder. Spatiotemporal hotspots of crime and disorder are examined to contextualize broken windows theory. Applications of multivariate modelling with shared components to ecological crime theories and crime prevention policy are discussed.

Keywords: spatiotemporal, shared component, multivariate, crime and disorder, Bayesian model

1. Introduction

Quantitative methods for spatial and spatiotemporal data generally analyze one outcome or dependent variable. Spatial methods for analyzing a single crime type at the small-area scale include mapping of crime rates, spatial regression models, and clustering algorithms such as local Moran's I and Getis-Ord G_i and G_i^* statistics (Ratcliffe and McCullagh, 1999; Anselin et al., 2000). To examine spatiotemporal crime change, studies have compared spatial crime clusters across two or more time periods (Frazier et al., 2013; He et al., 2017) and have used methods that analyze both geographic and temporal dimensions of a single crime type, including space-time interaction tests for point data, the space-time scan statistic for point and areal data, and generalized linear mixed models for areal data with spatial and temporal structure (Johnson and Bowers, 2004; Shiode and Shiode, 2014; Chun, 2014; Li et al., 2014).

Distinguishing the similarities and differences between the spatiotemporal patterns of multiple crime types is fundamental to theoretical development and crime prevention policy. If, for example, violent crime and property crime exhibit similar patterns, then both crime types may be associated with the same set of risk factors and explained by a generalizable theory (Weisburd et al., 1993). But if patterns are dissimilar, then crime prevention strategies should be designed for each type and type-specific theoretical explanations pursued (Haberman, 2017). Studies examining the patterns of multiple crime types often compare the results of separate analyses of a single crime type (e.g., the Knox test in Grubesic and Mack (2008) and the space-time scan statistic in Leitner and Helbich (2011)), however this approach does not account for the correlations between crime types or identify the patterns shared amongst two or more crime types.

Focusing on the spatiotemporal correlations between crime and disorder, broken windows theory contends that physical and social disorder, or physical signs of deterioration and unsettling behaviours, respectively, lead to increases in property crime and violent crime (Kelling and Wilson, 1982). Collective efficacy theory proposes that crime and disorder are associated with the same underlying social processes, but does not hypothesize that increases in disorder precede increases in crime (Sampson et al., 1997; Sampson and Raudenbush, 1999). While past research has shown that crime and disorder are correlated within neighborhoods (Skogan, 1990; Taylor, 2001; Yang, 2010), few studies have investigated how local patterns of crime and disorder change over time, explored if crime and disorder share one or more spatial or temporal patterns, or examined the degree to which disorder precedes crime at the small-area scale (Boggess and Maskaly, 2014; Shiode and Shiode, 2014).

This research applies a Bayesian multivariate modelling approach to analyze the spatiotemporal patterns of physical disorder, social disorder, property crime, and violent crime over five years at the small-area scale. Multivariate models simultaneously analyze multiple dependent variables and can accommodate data that are correlated between nearby areas, between adjacent time periods, and between outcomes. For dependent variables that have similar data-generating processes, multivariate models provide a framework for estimating shared components (or latent factors) that capture the spatial and/or temporal structure common to two or more of the dependent variables (Knorr-Held and Best, 2001; Richardson et al., 2006). In this study, three models with various assumptions regarding the spatial and temporal correlation structures between the four types of crime and disorder are compared. The best fitting model accounts for five demographic, socioeconomic, and built environment characteristics, and partitions the residuals of each crime and disorder type into one spatial shared component, one

temporal shared component, and type-specific spatial, temporal, and space-time components. The spatial shared component is found to explain the largest proportion of residual variability for all types of crime and disorder.

Following this introduction, methods for analyzing the spatiotemporal patterns of a single crime type are reviewed and broken windows, collective efficacy, and routine activity theories are outlined. Next, the case study data are described, three multivariate spatiotemporal models are detailed, and the best fitting model is identified. Results are visualized and interpreted, and the implications of this research for spatiotemporal analysis of small-area data, for ecological crime theories, and for crime prevention policy are discussed.

2. Methods for analyzing spatiotemporal crime patterns

Quantitative methods for analyzing spatiotemporal data can be grouped into three categories: space-time interaction tests, exploratory cluster detection techniques, and spatiotemporal modelling approaches (Robertson et al., 2010). Space-time interaction tests measure the clustering of a single outcome by comparing the observed number of point pairs that occur nearby in both space and time to the entire distribution of point pairs. The Knox test, for example, uses researcher-specified distance and time values to define space-time interaction, and has been applied to characterize the clustering of burglary, robbery, and assault, and to identify the distance and time thresholds indicative of repeat victimization (Knox and Bartlett, 1964; Grubesic and Mack, 2008). Space-time interaction tests are univariate and can be used to identify point pairs located within a given distance and time, but are not suitable for analyzing data aggregated at the small-area scale, multiple correlated outcomes, or covariates that may explain crime risk (Kim and O'Kelly, 2008; Shiode and Shiode, 2014).

2.1 Cluster detection techniques

Cluster detection techniques identify groups of points or areas with high or low crime (Anselin et al., 2000). Like space-time interaction tests, conventional cluster detection methods analyze one outcome and do not accommodate covariates. Three of the most popular local cluster detection methods applied to crime data are local Moran's I and Getis-Ord G_i and G_i^* statistics, all of which calculate an index of local spatial autocorrelation relative to a null hypothesis of spatial randomness for one time period (Getis and Ord, 1992; Anselin et al., 2000; Fotheringham, 2009). The spatial scan statistic also identifies points or areas with high crime by using a scanning window to calculate a test statistic based on observed and expected crime risk both within and outside of the scanning window (Kulldorff et al., 1998). While local Moran's I, Getis-Ord G_i and G_i^* statistics, and the spatial scan statistic are cross-sectional, they have been applied across multiple time periods to explore how the locations of violent crime and disorder hotspots change over time (Ceccato and Haining, 2004; Frazier et al., 2013; He et al., 2017).

Incorporating spatial and temporal information, the space-time scan statistic uses a scanning window with varying radii (space) and heights (time) to identify crime clusters for at least two time periods (Kulldorff et al., 1998). The space-time scan statistic has been used to explore seasonal violent crime clusters, monthly theft hotspots, and the impacts of a major hurricane on the location and duration of burglary and auto theft hotspots (Ceccato, 2005; Kim and O'Kelly, 2008; Nakaya and Yano, 2010; Leitner and Helbich, 2011). The space-time scan statistic has been adapted to accommodate network distances to better identify crime clusters at the address-level (Shiode and Shiode, 2014). Also exploring the space-time patterns of one crime type, Rey et al. (2012) develop a spatial Markov chain to estimate the probability that an area

will experience a crime event at a future time period conditional on initial levels of crime in immediate and adjacent areas.

2.2 Spatiotemporal modelling approaches

Within the framework of generalized linear mixed models (Breslow and Clayton, 1993), spatiotemporal modelling approaches analyze the associations between dependent and independent variables and include additional model terms to account for residual spatial and temporal structure (Waller et al., 1997; Chun, 2014). Spatiotemporal models used in past crime research have predominately analyzed one crime type as the dependent variable. In the frequentist statistical framework, one technique to account for spatial autocorrelation is eigenvector spatial filtering (ESF), which uses orthogonal and uncorrelated eigenvectors decomposed from spatial weights matrices to create a set of parameters with different spatial structures (Getis and Griffith, 2002; Tiefelsdorf and Griffith, 2007). Chun (2014) analyzes vehicle burglary over five years at the small-area scale, fitting Poisson and negative binomial regression models with ESF and autoregressive random effects to account for spatial and temporal structure, respectively. Exploring nonviolent crimes over five years, Helbich and Arsanjani (2015) also use Poison and negative binomial regression models with ESF and compare the models constructed for each time period to identify the eigenvectors that best account for global, regional, and local spatial patterns.

In the Bayesian statistical framework, residual spatial, temporal, and spatiotemporal structure is typically specified via prior distributions for random effects parameters. Briefly, Bayesian hierarchical models combine observed data and prior information (e.g., spatial and/or temporal adjacency) to estimate full probability distributions for model parameters. For small-

area data, the most common prior distribution used to model residual spatial structure is the intrinsic conditional autoregressive distribution (ICAR), which borrows information from nearby areas to estimate a spatially smoothed risk surface (Besag et al., 1991; see Section 5.1). With a temporal adjacency matrix, the ICAR prior distribution has also been applied to model non-linear time trends (Richardson et al., 2006; Quick et al., 2017). Past studies applying Bayesian spatiotemporal models to small-area crime data have analyzed violent crime and property crime over two years (Law et al., 2014; Law et al., 2015), burglary over four- and eight-year time periods (Li et al., 2013; Li et al., 2014), and police confidence over 36 quarters (Williams et al., 2018). Quick et al. (2018) use a Bayesian multivariate model to analyze burglary, robbery, vehicle crime, and violent crime, and identify two crime-general spatial patterns shared amongst all crimes and the three theft-related crimes.

3. Spatiotemporal theories of crime and disorder

Spatiotemporal patterns of crime and disorder are most commonly explained by broken windows and collective efficacy theories. Broken windows theory hypothesizes that high levels of physical and social disorder increase fear of crime amongst residents, signal to offenders that residents will not intervene in criminal behaviour, and lead to increases in both property crime and violent crime over time (Kelling and Wilson, 1982; Xu et al., 2005). By outlining the pathway from disorder to crime, broken windows theory has widely influenced public policy, motivating order-maintenance policing strategies that issue citations and arrests for non-criminal disorder incidents, such as loitering, panhandling, and graffiti, and urban planning guidelines that require remediation or demolition of abandoned buildings and vacant lots (Skogan, 1990; Sampson and Raudenbush, 2004; Harcourt and Ludwig, 2006; Hinkle and Weisburd, 2008).

Collective efficacy theory proposes that crime and disorder both result from low social cohesion and low informal social control (Sampson et al., 1997; Sampson and Raudenbush, 1999). Neighborhoods with low social cohesion and low informal social control, as operationalized by high socioeconomic disadvantage, high residential mobility, and high ethnic heterogeneity, are thought to exhibit high levels of crime and disorder because residents are ineffective at establishing and realizing common goals, such as living in a safe and orderly neighborhood (Sampson and Groves, 1989; Sampson et al., 1997; Laurence, 2017). Importantly, collective efficacy theory challenges the central tenet of broken windows theory that increases in disorder precede increases in crime and, instead, collective efficacy theory argues that crime and disorder are associated with the same underlying social processes and neighborhood conditions (Sampson and Raudenbush, 2004; Harcourt and Ludwig, 2006).

Despite the tensions between broken windows and collective efficacy theories being inherently spatiotemporal, past research has predominantly examined the relationships between one type of crime or disorder (as a single dependent variable) and other types of crime and disorder (as independent variables) for one time period (e.g., Sampson and Raudenbush, 2004; Cerda et al., 2009). Spatiotemporal analyses have observed that crime and disorder generally exhibit similar patterns (Doran and Lees, 2005; Yang, 2010; Boggess and Maskaly, 2014), however no study has explored if crime and disorder share an underlying spatial pattern, as hypothesized by collective efficacy theory, or investigated the degree to which disorder precedes crime at the small-area scale, as anticipated by broken windows theory.

In addition to broken windows and collective efficacy theories, intra-urban patterns of crime and disorder have been interpreted using routine activity theory. Routine activity theory hypothesizes that crime events occur when suitable targets, motivated offenders, and a lack of

capable guardianship converge in space and time (Cohen and Felson, 1979). By highlighting how the spatiotemporal distribution of suitable targets influences crime patterns, routine activity perspectives recognize that crime and disorder may be correlated in areas with many target types, such as in central business districts where both material goods for property crime and large populations for violent crimes are concentrated, but that crime and disorder may not be correlated in areas with only one target type, such as around a shopping mall where the number of property crime targets is likely greater than the number of violent crime targets.

4. Study region and data

The Region of Waterloo is composed of three municipalities (Cambridge, Kitchener, and Waterloo) and is located approximately 100 km west of Toronto, Ontario, Canada. The geographic unit of analysis was the census dissemination area (DA). DAs are the smallest areal unit that cover the entirety of Canada and are delineated such that residential populations are between 400 and 700. In the 2011 census there were 655 DAs in the study region with an average size of 0.49 km^2. A detailed map of the study region is shown in Appendix A.

Reported incident data for physical disorder, social disorder, property crime, and violent crime was obtained from Waterloo Regional Police Services for five years, from 2011 to 2015. Reported incident data are commonly used to measure both crime and disorder at the small-area scale (Braga and Bond, 2008; Yang, 2010). Physical disorder counts were the sum of property damage and graffiti incidents, and social disorder counts were the sum of drug, public mischief, public disturbance, indecent act, and intoxicated person incidents (Skogan, 1990; Hinkle and Weisburd, 2008). Property crime counts were the sum of break and enter, theft under $5,000, theft over $5,000, and motor vehicle theft incidents. Violent crime counts were the sum of

assault and robbery incidents. In total, there were 10,005 incidents of physical disorder, 12,338 incidents of social disorder, 46,856 property crimes, and 6,812 violent crimes. Descriptive statistics for the four types of crime and disorder are shown in Table 1.

Table 1. Descriptive statistics for total counts of crime and disorder and for five explanatory variables.

	Mean	SD
Crime and disorder types		
Physical disorder	15.27	21.37
Social disorder	16.84	47.97
Property crime	71.46	135.13
Violent crime	10.40	21.23
Explanatory variables		
Population	678.90	478.96
Residential mobility (%)	38.15	17.51
Low-income households (%)	12.61	11.69
Ethnic heterogeneity (0 to 1)	0.31	0.15
Central business district	0.02	NA [a]

[a] Standard deviation not reported for binary variables

Total counts of physical disorder, social disorder, property crime, and violent crime are mapped in Figure 1. In general, areas with high counts of all types of crime and disorder were located along the central commercial corridor as well as in the southwest and southeast of the

study region. Areas with high counts of violent crime were concentrated in close proximity to the central commercial corridor, whereas areas with high counts of physical disorder, social disorder, and property crime were relatively more dispersed.

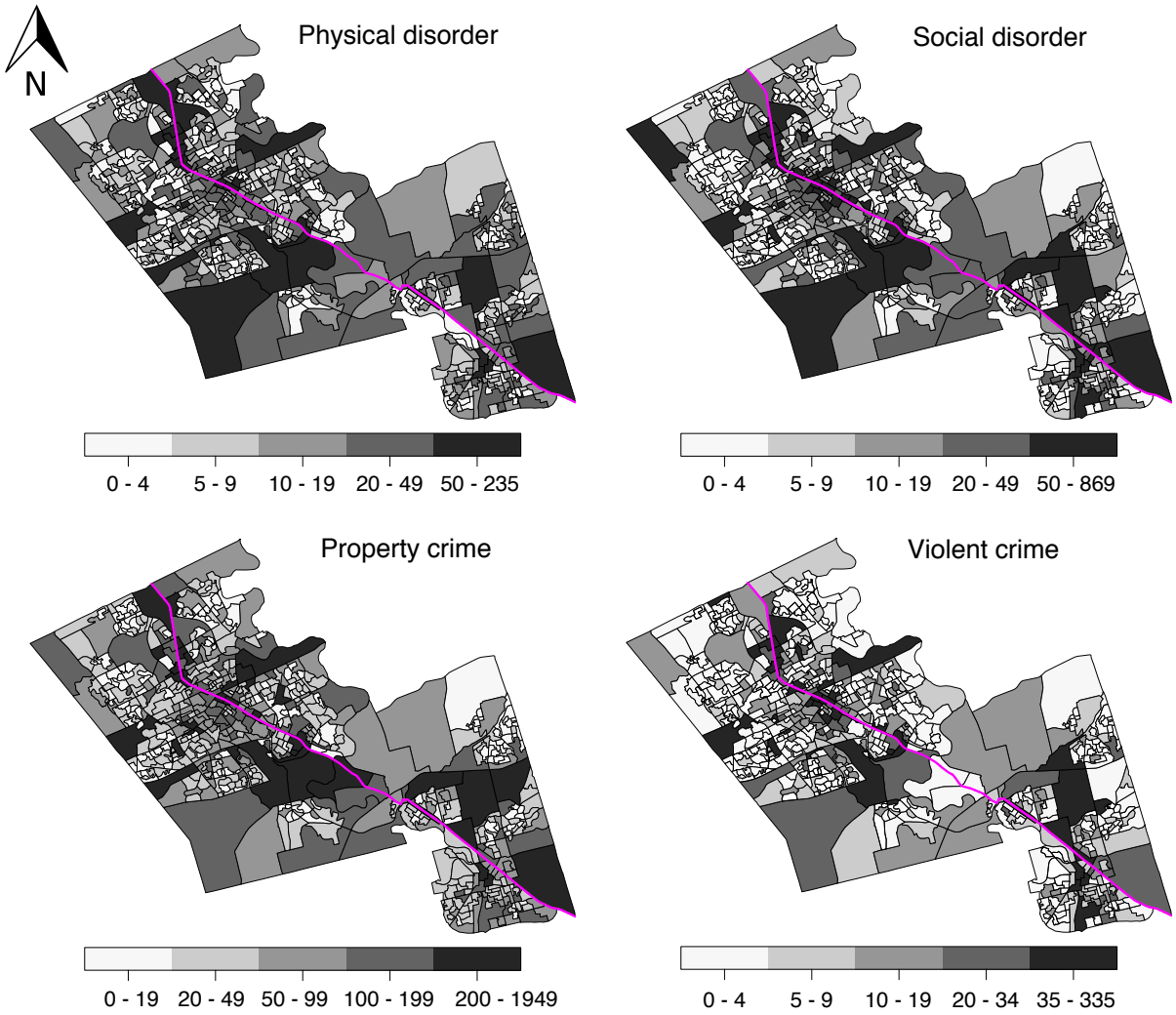

Figure 1. Total counts of physical disorder, social disorder, property crime, and violent crime. The central commercial corridor is highlighted.

Pairwise correlations between all types of crime and disorder were positive, confirming the visual similarities between crime and disorder maps. Social disorder and violent crime exhibited the strongest positive correlation (Kendall's $\tau_b = 0.70$ and Pearson's $r = 0.93$) while the weakest

positive correlations were between violent crime and property crime (Kendall's $\tau_b = 0.60$ and Pearson's $r = 0.62$) and between violent crime and physical disorder (Kendall's $\tau_b = 0.61$ and Pearson's $r = 0.58$). All types of crime and disorder were spatially autocorrelated as per a first-order queen contiguity spatial weights matrix ($p < 0.05$): social disorder had the highest spatial autocorrelation (Moran's I = 0.28), followed by violent crime (0.23), physical disorder (0.21), and property crime (0.14). Annual pairwise correlation coefficients and Moran's I values are shown in Appendix B.

Crime and disorder trends over the five-year study period are shown in Figure 2. In general, all types of crime and disorder decreased between 2011 and 2015, with physical disorder and social disorder showing modest and consistent declines across all years. Property crime increased slightly from 2011 to 2012, decreased during the third and fourth years, and increased by eight percent during the final year. Violent crime decreased by about 20% from 2011 to 2014 and increased by seven percent from 2014 to 2015.

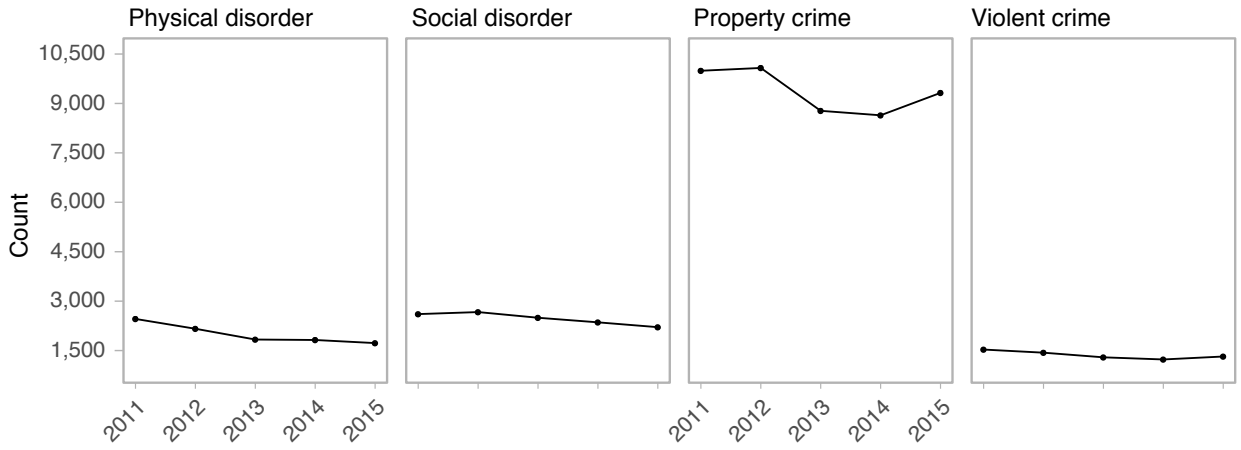

Figure 2. Annual counts of physical disorder, property crime, social disorder, and violent crime from 2011 to 2015.

Five explanatory variables operationalizing population size, socioeconomic context, and the built environment were analyzed (Table 1). Following Ceccato et al. (2018), residential population was included as an explanatory variable for two reasons. One, because there was no clear population at risk for the four types of crime and disorder. Two, because assuming that population size and crime/disorder are positively associated, which is implied when using residential population to derive crime/disorder rates (for continuous regression models) or offset terms (for count regression models), may not be appropriate, as past research has shown that crime/disorder often cluster in areas with small residential populations, such as in the central business district (Malleson and Andresen, 2015). Note that conceptualizing and measuring the population at risk in spatiotemporal analyses of crime/disorder is challenging because offenders and targets are mobile and because quantitative estimates of populations or crime targets are often not available (e.g., daytime populations) or accurately inferred using existing data at the small-area scale (e.g., the number of targets within a store).

The socioeconomic context of small-areas was operationalized via five-year residential mobility, the percent of low-income households, and the index of ethnic heterogeneity[1] (Sampson et al., 1997; Sturgis et al., 2014). These three variables are often used to characterize the structural dimensions of collective efficacy and have been found to be associated with crime and disorder at the small-area scale (Hinkle and Weisburd, 2008; Boggess and Maskaly, 2014).

[1] The index of ethnic heterogeneity for area $i = 1 - \sum h_{iz}^2$, where h_{iz} is the number of people of ethnicity z in area i divided by the total population in area i. The index of ethnic heterogeneity ranges between zero and one. Higher values of the index of ethnic heterogeneity indicate greater heterogeneity.

The central business districts (CBD) of the three municipalities were operationalized using a binary variable, where DAs within the CBDs were assigned a value of one and all other DAs were assigned a value of zero. This follows past research finding that crime and disorder incidents often cluster in and around the CBD (Sampson and Groves, 1989; Doran and Lees, 2005; Nelson et al., 2001). Residential population, residential instability, ethnic heterogeneity, and low-income household variables were standardized for analysis.

5. Multivariate spatiotemporal modelling of crime and disorder

Counts of each type of crime and disorder are denoted as O_{ijk}, where i indexes areas ($i = 1, \ldots, 655$), j indexes year ($j = 1, \ldots, 5$), and k indexes type ($k = 1, \ldots, 4$). We assume that O_{ijk} are independent Poisson variables conditional on mean μ_{ijk}; $O_{ijk} \sim \text{Poisson}(\mu_{ijk})$. The Poisson distribution is often used for Bayesian spatiotemporal modelling of small-area count data, where overdispersion and residual spatial and temporal correlations are accounted for via random effects parameters (Breslow and Clayton, 1993; Richardson et al., 2004; Haining et al., 2009).

Model 1 assumes no correlations between the four types of crime and disorder and models the Poisson means (μ_{ijk}) as the sum of a type-specific intercept (α_k), type-specific covariates for residential population, residential mobility, low-income households, ethnic heterogeneity, and the CBD ($\beta_{nk}x_{ni}$), a set of type-specific spatial random effects terms (s_{ik}), a set of type-specific temporal random effects terms (γ_{jk}), and a set of type-specific space-time random effects terms (θ_{ijk}). For the covariates ($n = 1, \ldots, 5$), the type-specific regression coefficients are represented by β_{nk} and the explanatory variable for each area is represented by x_{ni}. For each type of crime and disorder, the residual spatial pattern is captured by s_{ik}'s and the time trend is captured by γ_{jk}'s. The space-time random effects terms capture extra-Poisson variability not accounted for via

other model parameters and allow for the modeled counts of crime and disorder for each area and time period to depart from the stable spatial and temporal components (s_{ik} and γ_{jk}).

$$\log(\mu_{ijk}) = \alpha_k + \beta_{nk}x_{ni} + s_{ik} + \gamma_{jk} + \theta_{ijk} \quad (1)$$

Model 2 adds a spatial shared component for all types of crime and disorder and assumes that physical disorder, social disorder, property crime, and violent crime residuals share a common spatial pattern (MacNab, 2010). This is supported by visual similarities between maps of crime and disorder (Figure 1), positive pairwise correlations between all outcomes (Appendix B), and collective efficacy theory, which hypothesizes that crime and disorder are associated with the same geographically-varying social processes. The spatial shared component includes four type-specific factor loadings (λ_k) and a set of spatially structured random effects terms (f_i) (Knorr-Held and Best, 2001; Tzala and Best, 2008). The factor loadings allow each type of crime and disorder to have a unique association with the spatial pattern shared amongst all crime and disorder types (f_i). Type-specific spatial patterns that diverge from the shared spatial pattern are captured by s_{ik}'s.

$$\log(\mu_{ijk}) = \alpha_k + \beta_{nk}x_{ni} + (\lambda_k \cdot f_i) + s_{ik} + \gamma_{jk} + \theta_{ijk} \quad (2)$$

Model 3 adds a temporal shared component that captures the underlying time trend common to all four types of crime and disorder. A shared time trend is anticipated because all types of crime and disorder decreased over the five-year study period (Figure 2). The temporal shared component is the product of four type-specific temporal factor loadings (ϕ_k) and a set of temporally structured random effects terms (t_j). Like the spatial shared component, the temporal factor loadings quantify the relative association between each type of crime and disorder and the underlying shared time trend (t_j). Type-specific time trends that diverge from the shared trend are captured by γ_{jk}.

$$\log(\mu_{ijk}) = \alpha_k + \beta_{nk}x_{ni} + (\lambda_k \cdot f_i) + (\phi_k \cdot t_j) + s_{ik} + \gamma_{jk} + \theta_{ijk} \quad (3)$$

5.1 Prior distributions

In Bayesian modelling, all parameters are treated as random variables and assigned prior distributions. The type-specific intercepts (α_k) were each assigned improper uniform prior distributions (Thomas et al., 2004). The type-specific regression coefficients (β_{nk}) were each assigned a normal distribution with a mean of zero and variance of 1,000.

Random effects terms f_i, t_j, s_{ik}, γ_{jk}, and θ_{ijk} model the shared and type-specific spatial, temporal, and space-time structure of residuals after controlling for covariates. All random effects terms are estimated from the data. For the space-time random effects terms (θ_{ijk}), a centered parameterization was used to fit the models such that $\log(\mu_{ijk}) \sim \text{Normal}(\eta_{ijk}, \delta^2_{\theta_k})$, where $\eta_{ijk} = \alpha_k + \beta_{nk}x_{ni} + (\lambda_k \cdot f_i) + (\phi_k \cdot t_j) + s_{ik} + \gamma_{jk}$ (for Model 3) and where $\theta_{ijk} = \log(\mu_{ijk}) - \eta_{ijk}$ (Tzala and Best, 2008; Appendix E). This is equivalent to specifying θ_{ijk} as a set of unstructured random effects terms assigned normal prior distributions with means of zero and type-specific variances $\delta^2_{\theta_k}$. Centered parameterizations of generalized linear mixed models have been shown to improve convergence of random effects parameters fitted via Markov chain Monte Carlo (MCMC) algorithms (Gelfand et al., 1995).

The type-specific spatial random effects terms (s_{ik}) were assigned ICAR prior distributions with type-specific variances $\delta^2_{s_k}$. This prior assumes that crime and disorder residuals exhibit positive local spatial autocorrelation. In the ICAR distribution, each s_{ik} is normally distributed with the mean equal to the average of the means of s_{ik}'s in nearby areas (Besag et al., 1991). Spatial weights matrix W was used to define spatial adjacency for the ICAR prior distribution, where $W_{ii} = 0$, $W_{ic} = 1$ if area i is adjacent to area c, and $W_{ic} = 0$ otherwise (i.e., first-order queen

contiguity matrix). The conditional variances of the posterior distributions of s_{ik}'s are equal to $\delta^2_{s_k}$ / n_i, where n_i is the number of areas adjacent to area i, as defined in W. This assumes that areas with many neighbors will have more precise estimates of s_{ik} than areas with few neighbors (Besag et al., 1991).

In Models 2 and 3, the spatially structured random effects terms in the spatial shared component (f_i) were assigned ICAR prior distributions with the variance fixed to one (Hogan and Tchernis, 2004; Richardson et al., 2006; Tzala and Best, 2008). Because estimates obtained from MCMC chains may move between rotationally equivalent solutions at each iteration, fixing the variance to one guarantees a unique solution for spatial factor loadings (Hogan and Tchernis, 2004). Note that fixing the variance does not fix the posterior distributions of the f_i's. Spatial factor loadings (λ_k) were each assigned positive half-normal prior distributions with means of zero and variances of 1,000 (Tzala and Best, 2008). This assumes that all spatial factor loadings are positive, as indicated by the positive pairwise correlations between all outcomes (Appendix B). Note that, while specifying alternative numerical values for the fixed variance of shared components does change the scale of the factor loadings, it does not influence the degree to which each type of crime and disorder is explained by the model components. As such, the type-specific factor loadings are interpreted relative to each other. For example, the influence of the shared spatial pattern (f_i) on physical disorder is interpreted relative to the influence of the shared pattern on social disorder, and is quantified by λ_1 / λ_2.

Type-specific temporal random effects terms (γ_{jk}) were assigned ICAR prior distributions with type-specific conditional variances $\delta^2_{\gamma_k}$ and temporal weights matrix Q. Q was defined such that year j had adjacent time periods of $j + 1$ and $j - 1$, except for $j = 1$ and $j = 5$, which each had

only one adjacent time period (Thomas et al., 2004). This prior assumes that the time trends for each outcome were correlated between years (Richardson et al., 2006).

For the temporal shared component in Model 3, the logarithm of each factor loading was assigned a normal distribution with a mean of zero and a variance of 0.17 (i.e., $\log(\phi_k) \sim$ *Normal*(0, 0.17)). This assumes that all ϕ_k's are positive and that the temporal factor loadings range between 0.2 and 5 with 95% probability (Knorr-Held and Best, 2001). A sum-to-zero constraint was imposed on the $\log(\phi_k)$'s (Held et al., 2005). This prior distribution is more informative than the prior specified for the spatial factor loadings but was required for convergence of ϕ_k's, likely because there was little temporal variability of crime and disorder (see Table 3; Appendix D; Figure 6). A less informative prior distribution of *Normal*(0, 0.5) was also tested for the $\log(\phi_k)$'s with nearly identical results to those presented in Table 3. The common temporally structured random effects terms (t_j) were assigned ICAR prior distributions with temporal weights matrix *Q* and variances fixed to one to ensure model identifiability (Richardson et al., 2006; Tzala and Best, 2008). Like the spatial shared component, the magnitudes of the temporal factor loadings are interpreted relative to each other.

The standard deviations of type-specific random effects parameters (δ_{s_k}, δ_{γ_k}, and δ_{θ_k}) were assigned positive half-Gaussian prior distributions $Normal_{+\infty}(0, 10)$ (Gelman, 2006). To examine the sensitivity of the results to this prior, we tested *Gamma*(0.5, 0.0005) and *Gamma*(0.001, 0.001) distributions on the precisions of type-specific random effects and the results were similar to those presented here (Kelsall and Wakefield, 1999).

5.2 Model fitting, checking, and comparison

All models were fit using the MCMC algorithm in WinBUGS v.1.4.3. Two MCMC chains were initiated at dispersed starting values and the convergence of model parameters was monitored via trace plots and Gelman-Rubin diagnostics. Convergence was reached at 50,000 iterations. Posterior summaries were obtained from an additional 50,000 iterations, where every tenth iteration was retained to reduce autocorrelation of posterior samples. The Monte Carlo errors of model parameters were less than five percent of the corresponding standard deviations, which indicates that the total number of iterations (110,000) were sufficient to accurately estimate the posterior distributions of model parameters (Lunn et al., 2012).

Posterior predictive checks were used to test for potential discrepancies between the models and the observed data (Gelman et al., 1996). Ten thousand datasets (O^{rep}) were generated from Models 1, 2, and 3, and the probability that $O^{rep} \geq O$ was evaluated for four test statistics (T): the mean count, the standard deviation, the maximum count, and the skewness (Gilks et al., 1996). The probability $Pr(T(O^{rep}) \geq T(O))$ is referred to as the posterior predictive p-value. Posterior predictive p-values close to 0.5 indicate that the generated data are comparable to the observed data and p-values close to zero or one indicate a discrepancy between the model and the data. All models had posterior predictive p-values close to 0.5 for the four test statistics, showing that the generated data were consistent with the observed data (Appendix C).

Model fit was evaluated using the Deviance Information Criterion (DIC) and the Watanabe-Akaike Information Criterion (WAIC). The DIC and the WAIC both reward goodness of fit and penalize model complexity (Spiegelhalter et al., 2002; Gelman et al., 2014). While the DIC is the most common model fit criterion for Bayesian random effects models, it may under-penalize complex spatial models (Plummer, 2008). The WAIC has been proposed as an alternative measure of model fit that approximates leave-one-out cross-validation, a robust, albeit

computationally expensive, method for assessing model fit (Stern and Cressie, 2000; Gelman et al., 2014). For the DIC, smaller values indicate better fitting models and differences of five or greater are evidence of substantial model improvement (Lunn et al., 2012). For the WAIC, smaller values also indicate better fitting models and the difference between expected log pointwise predictive densities (with standard errors) can help to identify which model exhibits better fit (see Table 2) (Vehtari et al., 2017).

6. Results

Table 2 compares Models 1, 2, and 3 using the DIC and the WAIC. Compared to separately modelling the spatiotemporal patterns of each type of crime and disorder in Model 1, adding a spatial shared component in Model 2 resulted in improved model fit. Decreases in the DIC and the WAIC from Model 1 to Model 2 were attributable to both improved goodness of fit (smaller $\overline{D}$ and lpd_{WAIC}) and fewer effective parameters (smaller pD and p_{WAIC}). Adding a temporal shared component in Model 3 also led to smaller DIC and WAIC values, with improvements in goodness of fit at the expense of slightly greater model complexity. As per the DIC, neither Model 2 or Model 3 was favored as values were within five. As per the WAIC, the difference in the expected log pointwise predictive densities between Models 2 and 3 was 3.3 with a standard error of 2.0 in favor of Model 3. Focusing on the parameter estimates from Models 2 and 3, the posterior distributions of the parameters that explained the largest proportions of variability in both models were nearly identical (Figure 6; Appendix D), however the type-specific temporal components for all outcomes in Model 2 were greater than one during the first two years and less than one during the final two years. This qualitatively supports the common time trend included in Model 3. Therefore, Model 3 was chosen as the preferred model.

Table 2. DIC and WAIC results for the three multivariate spatiotemporal models.

Model	$\overline{D}$	pD	DIC [a]	lpd_{WAIC}	p_{WAIC}	WAIC [b]
1	44,263	4,265	48,528	-20,864	3,463	48,654
2	44,124	3,838	47,962	-20,919	3,085	48,008
3	44,117	3,842	47,959	-20,915	3,086	48,002

[a] DIC = $\overline{D}$ + pD, where $\overline{D}$ is the posterior mean of the deviance and pD is the effective number of parameters (Spiegelhalter et al., 2002).

[b] WAIC = -2($elpd_{WAIC}$), where $elpd_{WAIC}$ is the expected log pointwise predictive density. $elpd_{WAIC}$ = lpd_{WAIC} – p_{WAIC}, where lpd_{WAIC} is the log posterior predictive density and p_{WAIC} is the effective number of parameters (Gelman et al., 2014; Vehtari et al., 2017).

Table 3 shows the posterior medians and 95% credible intervals (95% CI) of the type-specific intercepts, the regression coefficients, the factor loadings, and the empirical variances of random effects terms from Model 3. The 95% CI is the interval that contains the true value of a parameter with 95% probability. Regression coefficients are shown as relative risks ($\exp(\beta_{nk})$) where values greater than one indicate positive associations between explanatory variables and crime/disorder. Residential population, residential mobility, and the central business district were found to be positively associated with all types of crime and disorder at 95% CI. This supports collective efficacy theory, which posits that crime and disorder are most frequent in areas where high residential mobility challenges the formation of social ties amongst residents and contributes to low informal social control (Sampson and Groves, 1989; Sampson et al., 1997; Boggess and Maskaly, 2014). These results also support past routine activity research showing

that crime and disorder disproportionately occur in downtown areas where offenders and potential targets converge during employment and leisure activities, and where the night-time economy is concentrated (Nelson et al., 2001).

Table 3. Posterior medians and 95% credible intervals of the intercept, regression coefficients, factor loadings, and empirical variances of random effects terms from Model 3.

	Physical disorder	Social disorder	Property crime	Violent crime
Intercept ($\exp(\alpha_k)$)	1.67 (1.61, 1.73)	1.30 (1.24, 1.35)	6.92 (6.77, 7.07)	0.78 (0.74, 0.82)
Residential population	1.33 (1.24, 1.43)	1.39 (1.26, 1.52)	1.34 (1.25, 1.44)	1.35 (1.23, 1.49)
Residential mobility	1.24 (1.13, 1.35)	1.27 (1.13, 1.42)	1.21 (1.10, 1.33)	1.26 (1.11, 1.41)
Low-income households	0.95 (0.88, 1.04)	1.01 (0.90, 1.12)	0.93 (0.85, 1.02)	1.02 (0.91, 1.15)
Ethnic heterogeneity	0.99 (0.92, 1.09)	1.00 (0.90, 1.12)	1.04 (0.96, 1.15)	0.97 (0.87, 1.10)
Central business district	1.65 (1.01, 2.68)	2.10 (1.14, 3.86)	1.63 (0.96, 2.65)	1.81 (0.97, 3.39)
Spatial factor loading	1.90 (1.77, 2.03)	2.60 (2.45, 2.77)	1.93 (1.80, 2.07)	2.57 (2.40, 2.75)
Temporal factor loading	1.18	0.78	1.08	1.00

	(0.66, 1.98)	(0.46, 1.53)	(0.60, 1.80)	(0.60, 1.68)
Empirical variances of random effects terms				
Spatial shared component: $\lambda_k \cdot f_i$	0.84 (0.74, 0.95)	1.58 (1.43, 1.75)	0.87 (0.77, 0.99)	1.54 (1.38, 1.74)
Temporal shared component: $\phi_k \cdot t_j$	0.02 (0, 0.05)	0.01 (0, 0.04)	0.006 (0, 0.05)	0.01 (0, 0.05)
Type-specific spatial: s_{ik}	0.13 (0.09, 0.17)	0.03 (0, 0.10)	0.23 (0.20, 0.27)	0.13 (0.08, 0.19)
Type-specific temporal: γ_{jk}	0.004 (0, 0.03)	0.001 (0, 0.02)	0.002 (0, 0.02)	0.001 (0, 0.02)
Type-specific space-time: θ_{ijk}	0.13 (0.10, 0.16)	0.07 (0.05, 0.09)	0.09 (0.07, 0.11)	0.08 (0.06, 0.12)

Factor loadings (λ_k and ϕ_k) quantify the relative associations between each type of crime and disorder and the shared spatial pattern (f_i) and the shared time trend (t_j) (Table 3). The magnitudes of factor loadings are interpreted relative to each other because the variances of f_i and t_j were fixed to one (Held et al., 2005). The spatial factor loadings for social disorder and violent crime were significantly greater than the loadings for physical disorder and property crime at 95% CI. Compared to physical disorder, which had the smallest spatial factor loading, the shared spatial pattern had a 1.37 times greater association with social disorder (2.60 / 1.90 = 1.37), a 1.35 times greater association with violent crime (2.57 / 1.90 = 1.35), and a similar magnitude of association with property crime (1.93 / 1.90 = 1.02). Temporal factor loadings had relatively greater positive associations with physical disorder, property crime, and violent crime

than with social disorder, however all temporal factor loadings had overlapping posterior distributions at 95% CI.

The shared spatial pattern ($\exp(f_i)$) and the shared time trend ($\exp(t_j)$) from Model 3 are visualized in Figure 3. The relative risk of the shared spatial pattern was highest along the central commercial corridor and lowest in areas west of the central commercial corridor and in areas around the periphery of the study region. This aligns with the visual similarities of the crime and disorder counts mapped in Figure 1. The shared time trend common to all outcomes decreased from 2011 to 2014, which is generally representative of the trend shown by the observed crime and disorder counts (Figure 2). The increase in the shared time trend from 2014 to 2015 is likely attributable to property crime as it was the most frequent dependent variable analyzed (Table 1).

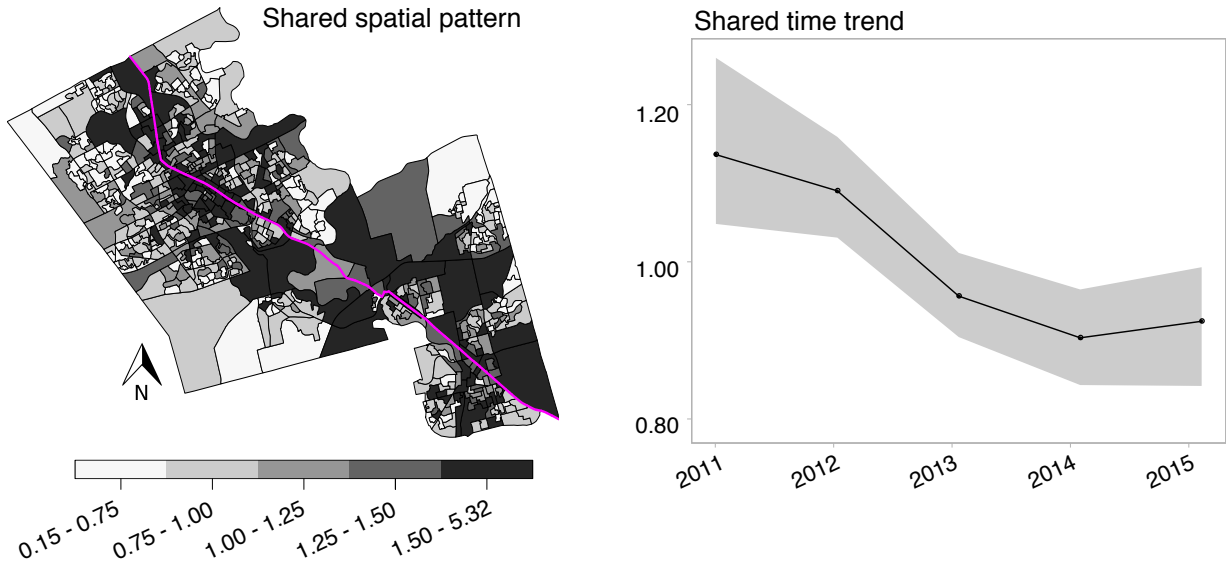

Figure 3. The shared spatial pattern and the shared time trend common to all types of crime and disorder. The 95% CI for the shared time trend is shaded grey.

Type-specific spatial patterns ($\exp(s_{ik})$) and time trends ($\exp(\gamma_{jk})$) are visualized in Figure 4 and Figure 5, respectively. Property crime had the largest empirical variance for the type-specific spatial component (= 0.23 (Table 3)) and exhibited the most heterogeneous spatial pattern, with areas of high risk located in the south and southeast of the study region. Social disorder had the smallest empirical variance for the type-specific spatial component (= 0.03) and exhibited a relatively uniform pattern throughout the study region. Physical disorder and violent crime had similar empirical variances for the type-specific spatial components but exhibited distinct patterns; areas with high type-specific risk of physical disorder were found in large clusters in the northwest and southeast of the study region, and areas with high type-specific risk of violent crime were located in smaller clusters near the central commercial corridor (Figure 4). The type-specific temporal components had the smallest empirical variances of all model parameters and the posterior distributions of $\exp(\gamma_{jk})$ were not unambiguously different from $\exp(t_j)$ at 95% CI (Figure 5). This suggests that the residual type-specific time trends were indistinguishable from the shared time trend.

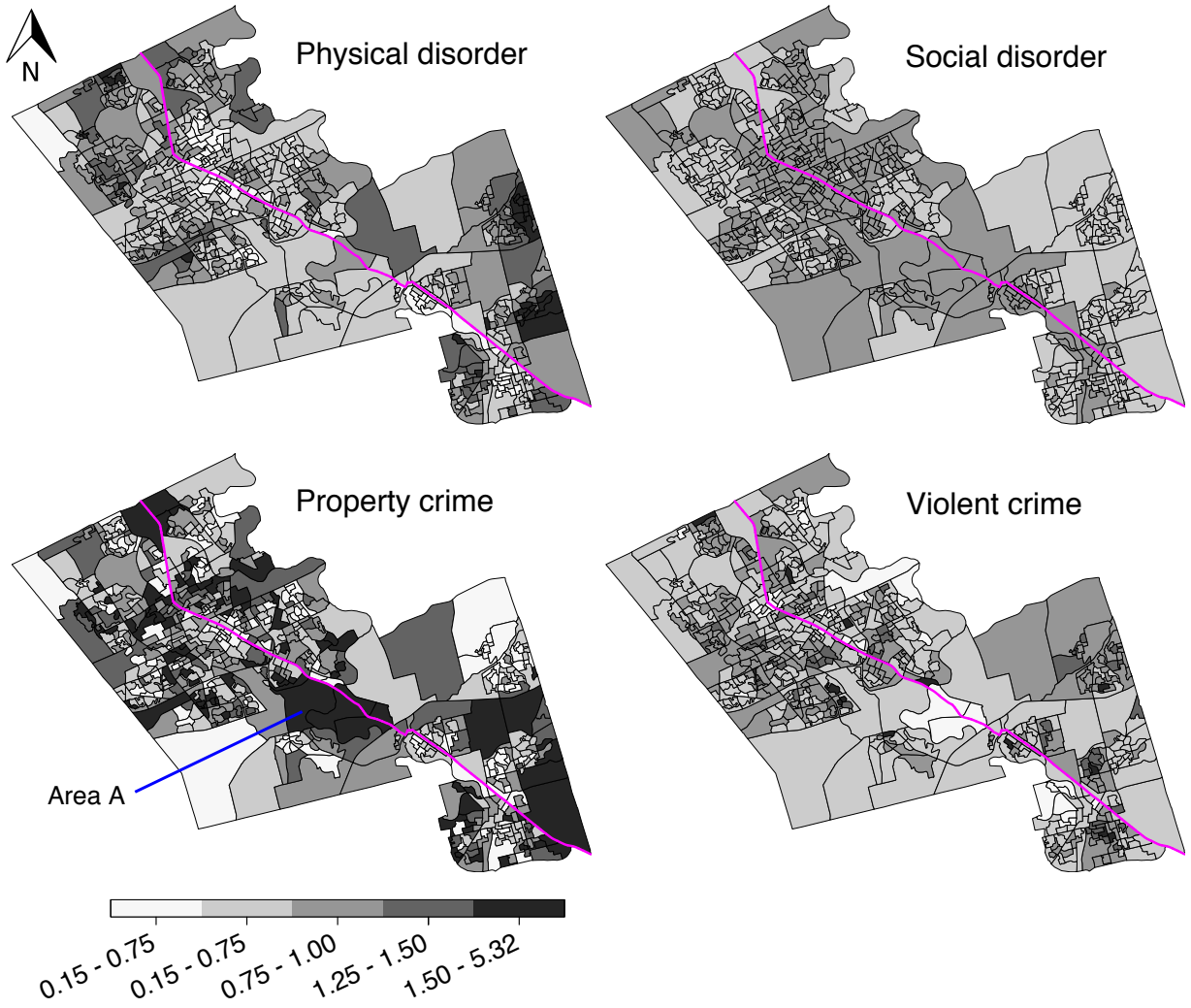

Figure 4. Type-specific spatial patterns for physical disorder, social disorder, property crime, and violent crime.

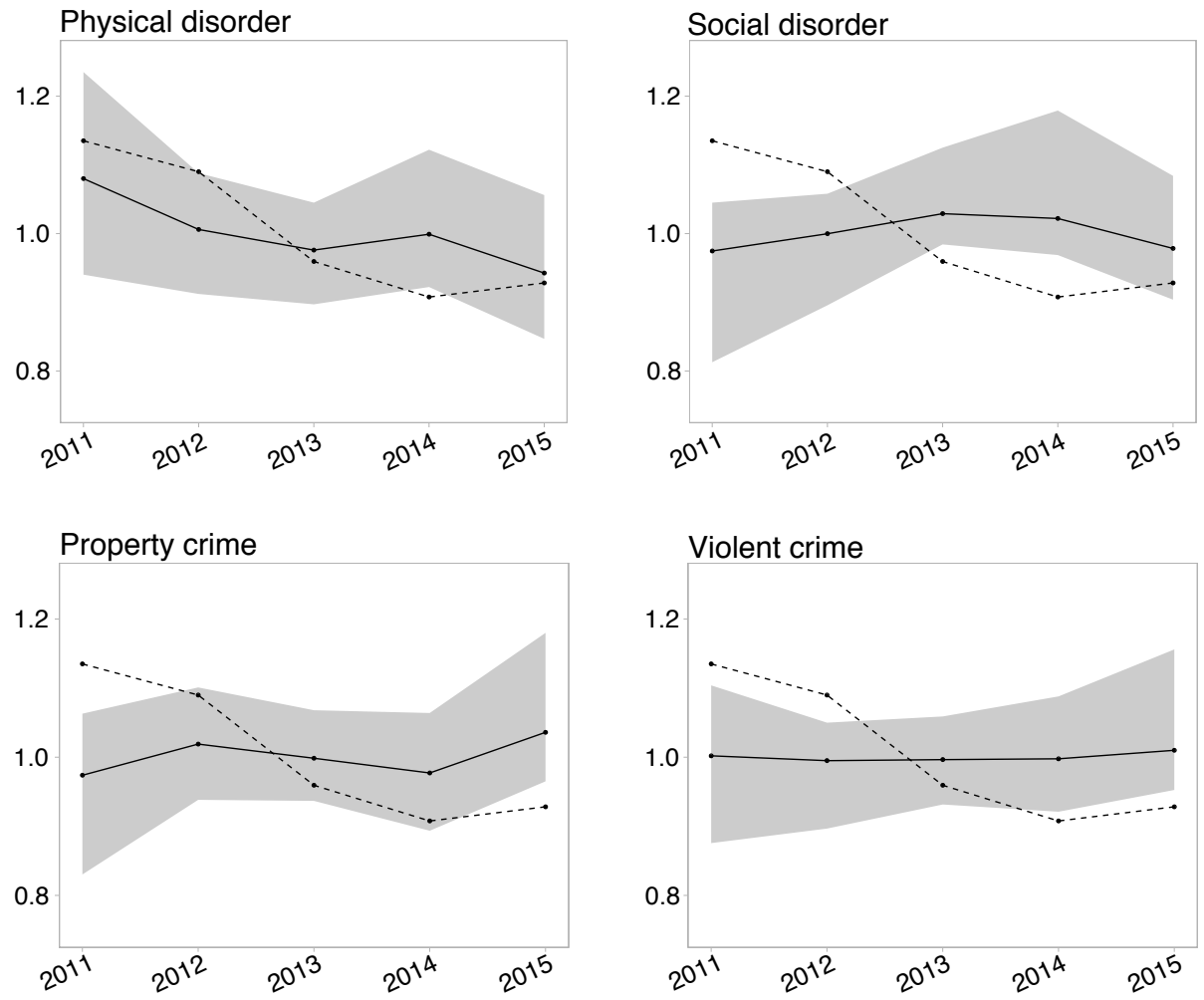

Figure 5. Type-specific time trends for physical disorder, social disorder, property crime, and violent crime. The 95% CIs for the type-specific time trends are shaded grey. The shared time trend is shown as a dashed line.

Variance partition coefficients (VPC) quantify the proportion of residual variability explained by shared and type-specific components for each crime and disorder type[2]. VPCs are

[2] For example, the VPC for the type-specific spatial component for physical disorder in Model 1 is the empirical variance of s_{i1} divided by the sum of the empirical variances of s_{i1}, γ_{j1}, and θ_{ij1}.

visualized in Figure 6 (see Appendix D for posterior medians and uncertainty intervals). In Model 1, the type-specific spatial components had the largest VPCs for all types of crime and disorder, however almost all of this variability was captured by the spatial shared component in Models 2 and 3. Indeed, the spatial shared component had the largest VPCs for all outcomes, accounting for approximately 93% of the residual variability of social disorder, 87% of violent crime, 75% of physical disorder, and 72% of property crime. Like the spatial shared component, the temporal shared component added in Model 3 captured almost all of the variability explained by the type-specific temporal components in Models 1 and 2 and, consequently, the type-specific temporal components had the smallest VPCs for all outcomes.

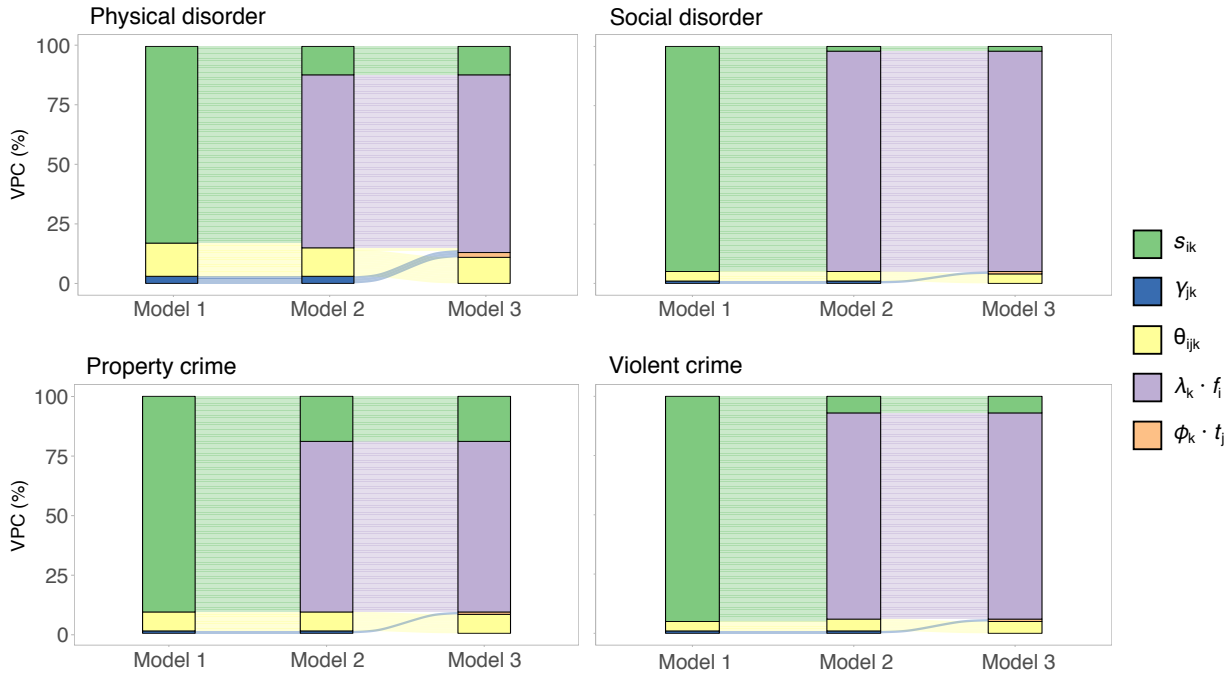

Figure 6. Variance partition coefficients for Models 1, 2, and 3.

6. Discussion

This article has applied a Bayesian multivariate modelling approach to analyze the spatiotemporal patterns of physical disorder, social disorder, property crime, and violent crime over five years at the small-area scale. Three models with different assumptions regarding the spatial and temporal correlation structures between the four outcomes were compared. The best fitting model accounted for five covariates operationalizing population size, socioeconomic context, and the central business district, and partitioned the residuals of each outcome into one spatial shared component, one temporal shared component, and four type-specific spatial, temporal, and space-time components. For all types of crime and disorder, the largest proportions of residual variability were explained by the spatial shared component and the smallest proportions of residual variability were explained by the type-specific temporal components.

Multivariate spatiotemporal models provide a framework for analyzing two or more correlated dependent variables that each exhibit spatial and temporal autocorrelation. In this research, the correlation structures between physical disorder, social disorder, property crime, and violent crime were estimated via one spatial shared component and one temporal shared component, which allow for each type of crime and disorder to be explained by a set of spatial random effects and a set of temporal random effects common to all outcomes (Knorr-Held and Best, 2001; Hogan and Tchernis, 2004). This research shows that adding shared components to capture the spatial pattern and time trend shared amongst all types of crime and disorder substantially improves model fit compared to analyses that assume that the spatiotemporal patterns of physical disorder, social disorder, property crime, and violent crime are not correlated with each other. Importantly, shared components are enabled by multivariate modelling of two or more dependent variables and are therefore overlooked when only one outcome is analyzed. For example, cluster detection techniques, which are the most common quantitative methods used to

compare the patterns of multiple crime types, typically analyze a single variable, do not accommodate covariates that may be associated with crime and disorder, and rely on researcher interpretation of hotspot locations and durations to infer the correlations between crime and disorder types (Leitner and Helbich, 2011; Haberman, 2017).

Conceptually, shared components represent latent risk factors that are simultaneously associated with two or more dependent variables (Held et al., 2005; MacNab, 2010). For physical disorder, social disorder, property crime, and violent crime, shared components are justified by broken windows and collective efficacy theories, both of which contend that crime and disorder are correlated within areas, between areas, and between time periods because they manifest from the same underlying social and behavioural processes (see Section 3). The results of this study show that, for all crime and disorder types, the spatial and temporal shared components explain larger proportions of residual variability than the corresponding type-specific parameters (Figure 6). This suggests that the shared spatial pattern and shared time trend are more important for understanding when and where crime and disorder occur than the separable type-specific patterns despite being overlooked in past research.

6.1 Multivariate modelling and collective efficacy theory

Enabled by join spatiotemporal modelling with shared components, this research provides novel insights for both ecological crime theories and policy applications. Focusing on theoretical inference, the regression coefficients and spatial factor loadings provide support for collective efficacy theory. In particular, residential mobility was found to be positively associated with all types of crime and disorder, and all spatial factor loadings were found to be unambiguously greater than zero (Table 3). This aligns with collective efficacy research observing that

neighborhoods with high residential mobility also have high levels of crime and disorder (Sampson and Raudenbush, 1999), but extends past studies by showing that, even after controlling for the structural characteristics operationalizing collective efficacy, all outcomes were positively associated with a common spatially structured latent risk factor (Table 3). This common risk factor had a significantly greater influence on social disorder and violent crime than on physical disorder and property crime, as indicated by the spatial factor loadings. In this context, the spatial shared component may capture dimensions of collective efficacy not measured via residential mobility, low-income households, and ethnic heterogeneity, for example peer group supervision or the degree to which residents will intervene in criminal behaviour (Sampson and Groves, 1989; Sampson et al., 1997).

Differentiating between the shared and type-specific components, physical disorder and property crime had relatively more heterogeneous type-specific spatial patterns and relatively larger VPCs for the type-specific space-time components than did social disorder and violent crime (Figure 4; Figure 6). One explanation for the greater divergence of physical disorder and property crime from the shared spatial pattern and the shared time trend is that, whereas social disorder and violent crime were predominately influenced by collective efficacy, as measured via the explanatory variables and the shared components, physical disorder and property crime were explained by collective efficacy as well as features of the built environment that were not included in this analysis (Sampson et al., 1997; Sampson and Raudenbush, 1999; Yang 2010). As highlighted by routine activity theory, physical features of the built environment, such as retail stores and infrastructure, are necessary for property crime and physical disorder incidents to occur. For example, the areas located in the southwest of the study region with high type-specific spatial risk of property crime (Area A in Figure 4), but low type-specific spatial risk of

all other outcomes, are near to a large shopping mall that provides many opportunities for property crimes but relatively fewer opportunities for incidents of violent crime or disorder.

6.2 Space-time hotspots, the broken windows theory, and policy applications

In addition to furthering the analysis of multiple correlated small-area outcomes and advancing theoretical inference, this multivariate modelling approach provides information regarding if, and how, areas with high levels of disorder transition to high levels of crime as proposed by broken windows theory. To date, little research has examined which types of disorder precede which types of crime after controlling for the effects of collective efficacy (i.e., the explanatory variables and the shared components). Hotspots of the type-specific space-time random effects terms were identified via the posterior probability $\Pr(\exp(\theta_{ijk}) > 1 \mid \text{data}) > 0.8$ (Richardson et al., 2004) and the number of disorder hotspots at time *j* that occurred one year prior to at least one crime hotspot in the same area or adjacent areas at time $j + 1$ were counted. Areal adjacency was determined via spatial weights matrix W (see Section 5.1). Boggess and Maskaly (2014) suggest that one year is an appropriate time frame for areas with high disorder to transition to high crime. Hotspot transitions are shown in Table 4.

In this case study, transitions from hotspots of social disorder or physical disorder to hotspots of property crime or violent crime were relatively infrequent (total of 297 over five years) compared to the number of small-areas analyzed (total of 3,275 over five years). The most common type of 'broken windows' transition was from hotspots of physical disorder to hotspots of property crime, accounting for nearly half of all hotspot transitions. Relative to the total number of disorder hotspots, however, the most prevalent type of transition was from social

disorder to property crime (64%). Substantially fewer social disorder or physical disorder hotspots transitioned to violent crime hotspots in the following year (Table 4).

Table 4. Areas that transition from disorder hotspots in year *j* to crime hotspots in year *j* + 1. The percentage of transition areas relative to the total number of disorder hotspots is shown in parentheses.

	Violent crime	Property crime
Social disorder	39 (34.8%)	72 (64.3%)
Physical disorder	48 (21.7%)	138 (60.1%)

Applied to policy, 'broken windows' transitions between hotspots of disorder to hotspots of crime suggest that law enforcement should scan for high levels of physical and social disorder and, in the next year, deploy geographically-focused crime prevention programs designed specifically to prevent property crime. Yet, because 'broken windows' transitions are relatively uncommon, and because the type-specific space-time components explain a smaller proportion of the overall variability than the spatial shared component for all four outcome types (Figure 6), it may be more effective for law enforcement resources and crime prevention policies to focus on centrally located neighborhoods with high residential mobility and with high risk due to the shared spatial pattern. That is, rather than implement policing strategies designed for a single crime type or deploy resources based on anticipated transitions from disorder to crime, programs and policies that target areas with consistently high risk due to the spatial shared component, and that attempt to increase informal social control and social cohesion, may have the largest impact on all types of crime and disorder (Sampson and Raudenbush, 2004; Haberman, 2017).

6.3 Limitations and future research

One limitation of this research is that crime and disorder data were obtained from a reported incident dataset and were retrieved from a single law enforcement agency. While reported incident data are commonly used in past research (Skogan, 1990; Braga and Bond, 2008; Yang, 2010), it is possible that the correlations between outcomes reflect, in part, the existing distribution of police resources or data misclassification between related incidents, such as physical disorder and property crime (Nelson et al., 2001). A second limitation is that the spatial shared component, which specifies an ICAR prior distribution for the common spatially structured random effects terms, assumes that the shared pattern exhibits local spatial autocorrelation and that the shared pattern, as well as the relative influence of the shared pattern on all outcomes, is stable over time (Knorr-Held and Best, 2001). However, it is possible that the correlation structures between outcomes can be similar amongst groupings of non-adjacent areas, and that the shared pattern and the factor loadings can change over time. One method to explore in future research is profile regression modelling, which can identify groups of adjacent and non-adjacent small-areas with similar relative risks of multiple outcomes (Liverani et al., 2016). Studies should also explore the methodological and practical implications of allowing the correlation structure between outcomes to change over space and/or time, perhaps by estimating space- or time-varying factor loadings. Third, we include three covariates to operationalize collective efficacy at the small-area scale, however recent studies have shown that the relationships between neighborhood structural characteristics and social processes are contextual and interact with broader patterns of diversity and segregation (Sturgis et al., 2014; Laurence, 2017). Future studies may look to apply this multivariate modelling approach at multiple spatial

scales, exploring if regression coefficients and shared components are consistent across scales and examining how shared components change after controlling for socio-spatial processes operating at larger areal units.

Future research should also investigate how shared and type-specific patterns of crime and disorder evolve over shorter and longer time periods. For shorter temporal units, such as months, this method would be helpful in evaluating the effects of policing tactics on all, or only a subset, of crime outcomes. For longer time periods, such as decades, multivariate spatiotemporal modelling can be used to explore how processes of urban change lead to increases or decreases in multiple crime and disorder types. If analyzing counts of specific crime types, future research should consider different operationalizations of population at risk. For crime types such as residential burglary, the number of dwellings can be incorporated into Poisson models as an offset (e.g., Li et al., 2014), however for more ambiguous crime types such as violent and property crimes, supplementing the residential population with quantitative estimates of the daytime population and the prevalence of night-time activities may be informative.

Appendix A: Detailed map of the study region.

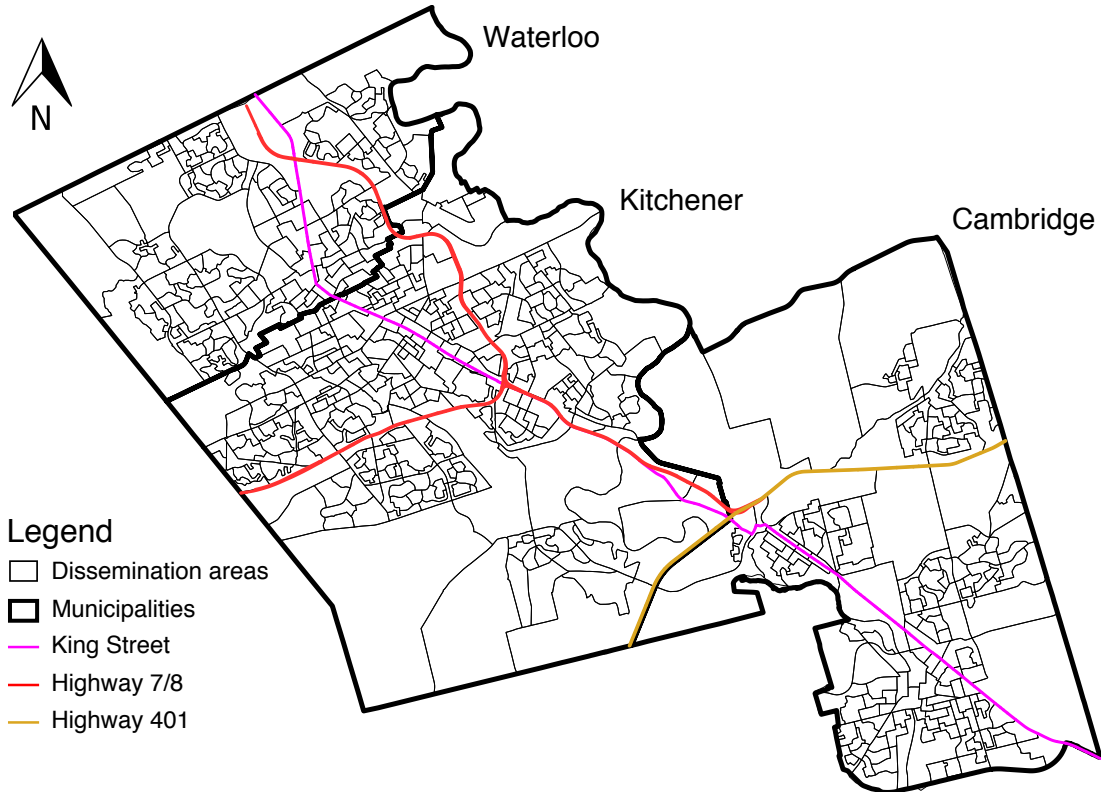

Appendix B: Annual Moran's I and pairwise correlation coefficients.

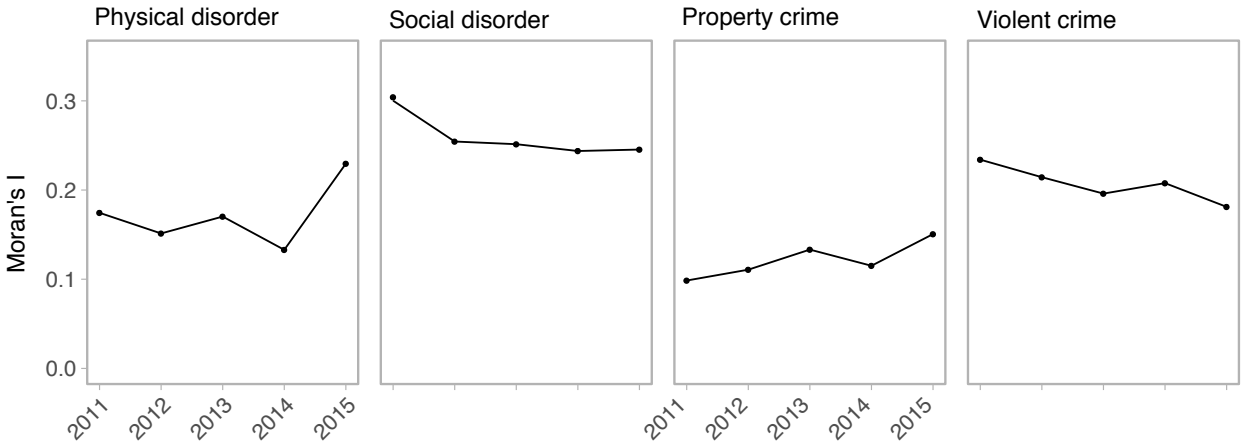

Figure B1. Annual Moran's I values for crime and disorder.

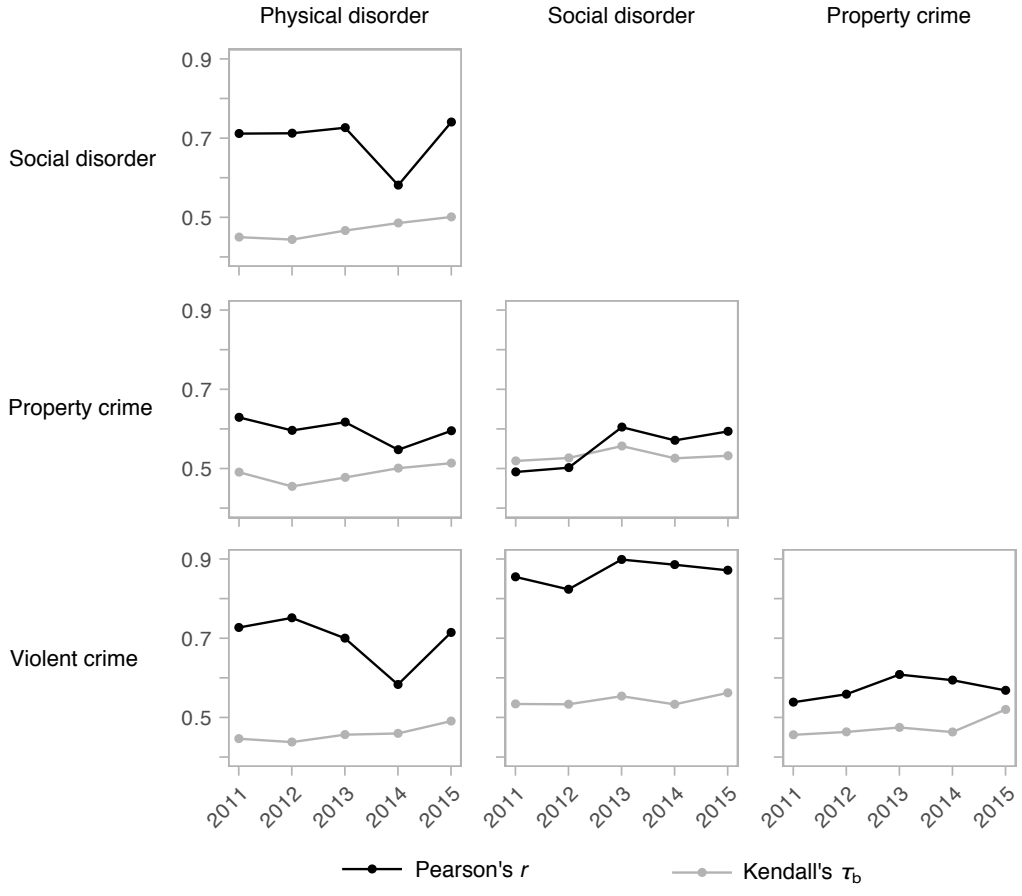

Figure B2. Annual pairwise correlation coefficients for crime and disorder counts.

Appendix C: Posterior predictive distributions and p-values.

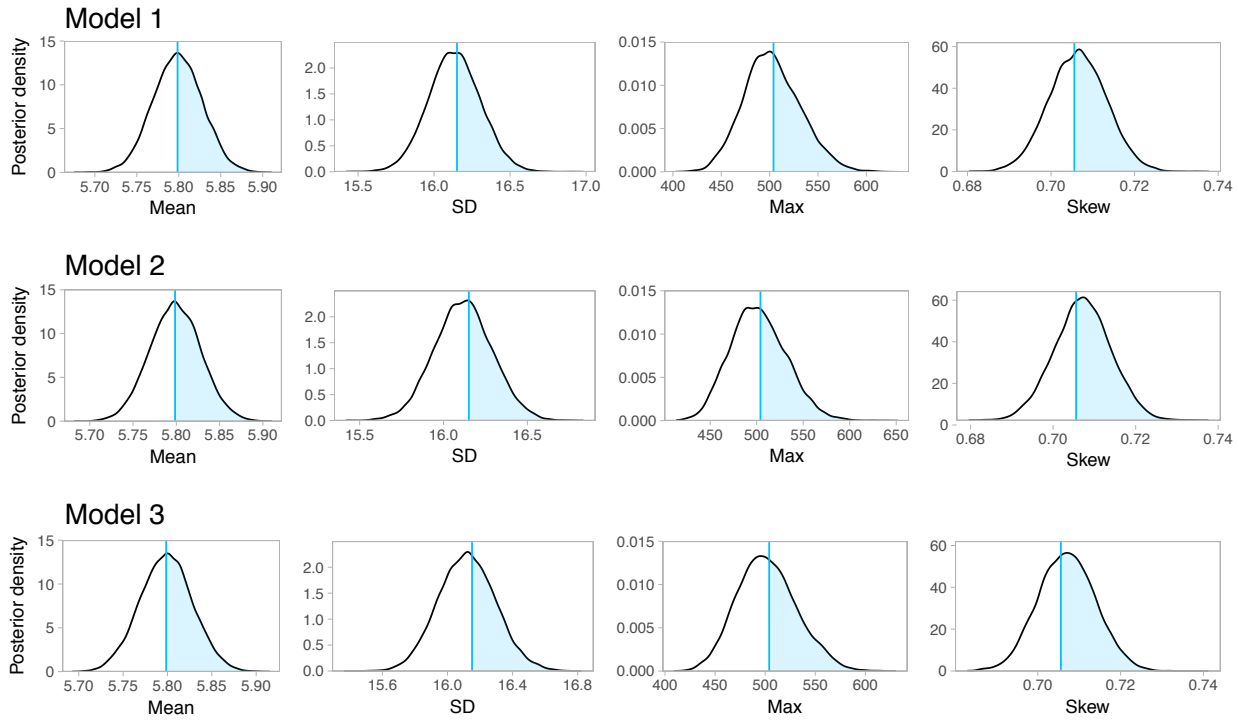

Figure C. Posterior predictive distributions for Models 1, 2, and 3. The shaded regions correspond to the posterior predictive p-values.

Table C. Posterior predictive p-values for Models 1, 2, and 3.

	Mean	SD	Max	Skew
Model 1	0.50	0.46	0.46	0.55
Model 2	0.50	0.42	0.45	0.59
Model 3	0.50	0.43	0.46	0.58

Appendix D: Variance partition coefficients for Models 1, 2, and 3. Posterior medians and 95% credible intervals are shown.

Model 1: Type-specific spatial, temporal, and space-time components.

	Physical disorder	Social disorder	Property crime	Violent crime
s_{ik}	83.46 (80.23, 86.46)	95.61 (93.84, 97.12)	90.74 (89.08, 92.29)	95.04 (92.88, 96.88)
γ_{jk}	3.00 (1.44, 4.63)	0.28 (0, 1.45)	1.08 (0, 2.26)	0.57 (0, 1.80)
θ_{ijk}	13.50 (10.74, 16.53)	4.09 (2.56, 5.84)	8.17 (6.63, 9.73)	4.38 (2.59, 6.47)

Model 2: Spatial shared component and type-specific spatial, temporal, and space-time components.

	Physical disorder	Social disorder	Property crime	Violent crime
s_{ik}	11.76 (8.50, 14.94)	1.85 (0, 6.43)	19.27 (16.52, 22.28)	7.55 (4.62, 10.81)
γ_{jk}	2.49 (1.00, 4.00)	0.26 (0, 1.39)	0.97 (0, 2.16)	0.55 (0, 1.76)
θ_{ijk}	11.40 (8.90, 14.20)	3.90 (2.36, 5.55)	7.44 (5.87, 9.01)	4.68 (2.70, 6.88)
$\lambda_k \cdot f_i$	74.33 (70.80, 77.83)	93.92 (89.45, 96.54)	72.30 (68.91, 75.40)	87.14 (83.91, 90.05)

Model 3: Spatial shared component, temporal shared component, and type-specific spatial, temporal, and space-time components.

	Physical disorder	Social disorder	Property crime	Violent crime
s_{ik}	11.62 (8.43, 14.85)	2.05 (0.01, 6.40)	19.26 (16.48, 22.46)	7.50 (4.71, 10.84)
γ_{jk}	0.41 (0, 2.45)	0.10 (0, 1.76)	0.24 (0, 1.90)	0.06 (0, 1.49)
θ_{ijk}	11.54 (8.95, 14.44)	3.96 (2.36, 5.57)	7.44 (5.88, 9.07)	4.76 (2.86, 6.91)
$\lambda_k \cdot f_i$	74.63 (70.51, 78.06)	93.13 (88.36, 95.91)	71.74 (67.34, 75.00)	86.81 (82.64, 89.87)
$\phi_k \cdot t_j$	1.45 (0, 4.71)	0.37 (0, 2.59)	1.08 (0, 4.06)	0.61 (0, 2.89)

Appendix E: WinBUGS code for Model 3.

```
model {
for (i in 1:N){              ### N is areas
for (j in 1:J) {             ### J is time periods
for (k in 1:K) {             ### K is crime/disorder types

O[i,j,k] ~ dpois(mu[i,j,k])

### centered parameterization of log(mu[i,j,k])
log(mu[i,j,k]) <- log.mu[i,j,k]
log.mu[i,j,k] ~ dnorm(eta[i,j,k], tau.theta[k])
eta[i,j,k] <- alpha[k] + s[k,i] + gamma[k,j] + (lambda[k] * f[i]) + (phi[k] * t[j]) + (beta1[k] * popcount[i]) +
(beta2[k] * lowinc[i]) + (beta3[k] * mov[i]) + (beta4[k] * ieh[i]) + (beta5[k] * cbd[i])

### calculate space-time parameters (theta[i,j,k])
theta[i,j,k] <- log.mu[i,j,k] - eta[i,j,k]
}}}

###### PARAMETERS ########################################
# alpha[k] = intercepts          s[k,i] = type-specific spatial random effects       beta[k]'s = coefficients
# gamma[k,j] = type-specific temporal random effects     lambda[k] = loading for spatial shared component
# f[i] = shared spatial random effects       t[j] = shared temporal random effects
# phi[k] = loading for temporal shared component    theta[I,j,k] = spatiotemporal random effects
### shared time trend
for (k in 1:K){
   logphi[k] ~ dnorm(0, 5.9)
   logphi.c[k] <- logphi[k] - mean.phi
   phi[k] <- exp(logphi.c[k])
}
mean.phi <- mean(logphi[1:4])
for (p in 1:sumNumNeigh.t) {    weights.t[p] <- 1    }          ### set weights for temporal ICAR
t[1:J] ~ car.normal(adj.t[], weights.t[], num.t[], 1)
for (j in 1:J) {    exp.t[j] <- exp(t[j])    }

### shared spatial pattern
for (p in 1:sumNumNeigh.s) {    weights.s[p] <- 1    }        ### set weights for spatial ICAR
f[1:N] ~ car.normal(adj.s[], weights.s[], num.s[], 1)
for (k in 1:K) {    lambda[k] ~ dnorm(0, 0.001)I(0, )    }

### type-specific spatial patterns and time trends
for (k in 1:K) {
s[k, 1:N] ~ car.normal(adj.s[], weights.s[], num.s[], tau.s[k])
gamma[k, 1:J] ~ car.normal(adj.t[], weights.t[], num.t[], tau.gamma[k])
}

### set priors for intercepts, coefficients, and set hyperpriors for random effects terms
for (k in 1:K) {
   tau.theta[k] <- 1 / pow(sd.theta[k], 2);    sd.theta[k] ~ dnorm(0, 10)I(0, )
   alpha[k] ~ dflat()
   beta1[k] ~ dnorm(0, 0.001);    beta2[k] ~ dnorm(0, 0.001);    beta3[k] ~ dnorm(0, 0.001)
   beta4[k] ~ dnorm(0, 0.001);    beta5[k] ~ dnorm(0, 0.001)
   tau.s[k] <- 1 / pow(sd.s[k], 2);     sd.s[k] ~ dnorm(0, 10)I(0,)
   tau.gamma[k] <- 1 / pow(sd.gamma[k], 2);     sd.gamma[k] ~ dnorm(0, 10)I(0,)
}}
```

References

Anselin, L., J. Cohen, D. Cook, W. Gorr, and G. Tita. (2000). "Spatial analyses of crime." *Criminal Justice* 4(2), 213–62.

Besag, J., J. York, and A. Mollie. (1991) "Bayesian image restoration with two applications in spatial statistics." *Annals of the Institute of Statistical Mathematics* 43(1), 1–20.

Boggess, L. N. and J. Maskaly. (2014). "The spatial context of the disorder-crime relationship in a study of Reno neighborhoods." *Social Science Research* 43, 168–83.

Braga, A. A. and B. J. Bond. (2008). "Policing crime and disorder hot spots: A randomized controlled trial." *Criminology* 46(3), 577–607.

Breslow, N. E. and D. G. Clayton. (1993). "Approximate inference in generalized linear mixed models." *Journal of the American Statistical Association* 88(421), 9–25.

Ceccato, V. (2005). "Homicide in Sao Paulo, Brazil: Assessing spatial-temporal and weather variations." *Journal of Environmental Psychology* 25, 307–21.

Ceccato, V. and R. Haining. (2004). "Crime in border regions: The Scandinavian case of Oresund, 1998–2001." *Annals of the Association of American Geographers* 94, 807–26.

Ceccato, V., G. Li, and R. Haining. (2018). "The ecology of outdoor rape: The case of Stockholm, Sweden." *European Journal of Criminology*, DOI: 10.1177/1477370818770842

Cerda, M., M. Tracy, S. F. Messner, D. Vlahov, K. Tardiff, and S. Galea. (2009). "Misdemeanor policing, physical disorder, and gun-related homicide." *Epidemiology* 20(4), 533–41.

Chun, Y. (2014). "Analyzing space-time crime incidents using eigenvector spatial filtering: An application to vehicle burglary." *Geographical Analysis* 46(2), 165–84.

Cohen, L. W and M. Felson. (1979). “Social change and crime rate trends: A routine activity approach.” *American Sociological Review* 44(4), 588–608.

Doran, B. J. and B. G. Lees. (2005). “Investigating the spatiotemporal links between disorder, crime, and the fear of crime.” *The Professional Geographer* 57(1), 1–12.

Fotheringham, A. S. (2009). “‘The problem of spatial autocorrelation’ and local spatial statistics.” *Geographical Analysis* 41(4), 398–403.

Frazier, A. E., S. Bagchi-Sen, and J. Knight. (2013). “The spatio-temporal impacts of demolition land use policy and crime in a shrinking city.” *Applied Geography* 41, 55–64.

Gelfand, A. E., S. K. Sahu, and B. P. Carlin. (1995). Efficient parametrisations for normal linear mixed models. *Biometrika* 82(3), 479–88.

Gelman, A., X-L. Meng and H. Stern. (1996). “Posterior predictive assessment of model fitness via realized discrepancies.” *Statistica Sinica* 6(4), 733–60.

Gelman, A. (2006). “Prior distributions for variance parameters in hierarchical models.” *Bayesian Analysis* 1(3), 515–33.

Gelman, A., J. Hwang, and A. Vehtari. (2014). “Understanding predictive information criterion for Bayesian models.” *Statistical Computing* 24, 997–1016.

Getis, A. and J. K. Ord. (1992). “The analysis of spatial association by use of distance statistics.” *Geographical Analysis* 24(3), 189–206.

Getis, A. and D. A. Griffith. (2002). “Comparative spatial filtering in regression analysis.” *Geographical Analysis* 34(2), 130–40.

Gilks, W. R, S. Richardson and D. J. Spiegelhalter. (2006). Markov Chain Monte Carlo in practice. Dordrecht: Springer Science.

Grubesic, T. H. and E. A. Mack. (2008). "Spatio-temporal interaction of urban crime." *Journal of Quantitative Criminology* 24, 285–306.

Haberman, C. P. (2017). "Overlapping hot spots? Examination of the spatial heterogeneity of hot spots of different crime types." *Criminology and Public Policy* 16(2), 633–60.

Haining, R., J. Law, and D. Griffith. (2009). "Modelling small area counts in the presence of overdispersion and spatial autocorrelation." *Computational Statistics and Data Analysis* 53, 2923–37.

Harcourt, B. E. and J. Ludwig. (2006). "Broken windows: New evidence from New York City and a five-city social experiment." *The University of Chicago Law Review* 73(1), 271–320.

He, L., A. Paez, and D. Liu. (2017). "Persistence of crime hot spots: An ordered probit analysis." *Geographical Analysis* 49(1), 3–22.

Helbich, M. and J. J. Arsanjani. (2015). "Spatial eigenvector filtering for spatiotemporal crime mapping and spatial crime analysis." *Cartography and Geographic Information Science* 42(2), 134–48.

Held, L., I. Natario, S. E. Fenton, H. Rue, and N. Becker. (2005). "Towards joint disease mapping." *Statistical Methods in Medical Research* 14, 61–82.

Hinkle, J. and D. Weisburd. (2008). "The irony of broken windows policing: A micro-place study of the relationship between disorder, focused police crackdowns and fear of crime." *Journal of Criminal Justice* 36, 503–12.

Hogan, J. W. and R. Tchernis. (2004). "Bayesian factor analysis for spatially correlated data, with application to summarizing area-level material deprivation from census data." *Journal of the American Statistical Association* 99(466), 314–24.

Johnson, S. D. and K. J. Bowers. (2004). "The stability of space-time clusters of burglary." *British Journal of Criminology* 44, 55–65.

Kelling, G. L. and J. Q. Wilson. (March 1982). "Broken windows." *The Atlantic Magazine*.

Kelsall, J. E. and J. C. Wakefield. (1999). "Discussion of 'Bayesian models for spatially correlated disease and exposure data' by Best N. G., R. A. Arnold, A. Thomas, L. Waller, and E. M. Conlon." In *Bayesian Statistics 6*, 131–56, edited by J. M. Bernardo, J. O. Berger, P. Dawid, and A. F. M. Smith. Oxford: Oxford University Press.

Kim, Y. and M. O'Kelly. (2008). "A bootstrap based space-time surveillance model with an application to crime occurrences." *Journal of Geographical Systems* 10, 141–65.

Knorr-Held, L. and N. G. Best. (2001). "A shared component model for detecting joint and selective clustering of two diseases." *Journal of the Royal Statistical Society, Series A: Statistics in Society* 164(1), 73–85.

Knox, E.G. and M. S. Bartlett. (1964). "The detection of space-time interactions." *Journal of the Royal Statistical Society, Series C: Applied Statistics*, 13(1), 25–30.

Kulldorff, M., W. F. Athas, E. J. Feuer, B. A. Miller, and C. R. Key (1998). "Evaluating cluster alarms: A space-time scan statistic and brain cancer in Los Alamos, New Mexico." *American Journal of Public Health* 88(9), 1377–80.

Laurence, J. (2017). "Wider-community segregation and the effect of neighbourhood ethnic diversity on social capital: An investigation into intra-neighbourhood trust in Great Britain and London." *Sociology* 51(5), 1011–33.

Law, J., M. Quick, and P. W. Chan. (2014). "Bayesian spatio-temporal modeling for analyzing local patterns of crime over time at the small-area level." *Journal of Quantitative Criminology* 30(1), 57–78.

Law, J., M. Quick, and P. W. Chan. (2015). "Analyzing hotspots of crime using a Bayesian spatio-temporal modeling approach: A case study of violent crime in the Greater Toronto Area." *Geographical Analysis* 47(1), 1–19.

Leitner, M. and M. Helbich (2011). "The impact of hurricanes on crime: A spatio-temporal analysis in the City of Houston, Texas." *Cartography and Geographic Information Science* 38(2), 213–21.

Li, G., R. Haining, S. Richardson, and N. Best. (2013). "Evaluating the No Cold Calling zones in Peterborough, England: Application of a novel statistical method for evaluating neighbourhood policing policies." *Environment and Planning A* 45, 2012–16.

Li, G., R. Haining, S. Richardson, and N. Best. (2014). "Space-time variability in burglary risk: A Bayesian spatio-temporal modelling approach." *Spatial Statistics* 9, 180–91.

Liverani, S., A. Lavigne, and M. Blangiardo. (2016). "Modelling collinear and spatially correlated data." *Spatial and Spatio-temporal Epidemiology* 18, 63–73.

Lunn, D., C. Jackson, N. Best, A. Thomas, and D. Spiegelhalter. (2012). *The BUGS Book: A practical introduction to Bayesian analysis*. London: Chapman and Hall/CRC Press.

MacNab, Y. C. (2010). "On Bayesian shared component disease mapping and ecological regression with errors in covariates." *Statistics in Medicine* 29, 1239–49.

Malleson, N. and M. A. Andresen. (2015). "The impact of using social media data on crime rate calculations: Shifting hotspots and changing spatial patterns." *Cartography and Geographic Information Science* 42(2), 112–21.

Nakaya, T. and K. Yano (2010). "Visualising crime clusters in a space-time cube: An exploratory data-analysis approach using space-time kernel density estimation and scan statistics." *Transactions in GIS* 14(3), 223–29.

Nelson, A. L., R. D. F. Bromley, and C. J. Thomas. (2001). "Identifying micro-spatial and temporal patterns of violent crime and disorder in the British city centre." *Applied Geography* 21, 249–74.

Plummer, M. (2008). "Penalized loss functions for Bayesian model comparison." *Biostatistics* 9(3), 523–39.

Quick, M., J. Law, and G. Li. (2017). "Time-varying relationships between land use and crime: A spatio-temporal analysis of small-area seasonal property crime trends." *Environment and Planning B: Urban Analytics and City Science*, DOI: 10.1177/2399808317744779.

Quick, M., G. Li, and I. Brunton-Smith. (2018). "Crime-general and crime-specific spatial patterns: A multivariate spatial analysis of four crime types at the small-area scale." *Journal of Criminal Justice* 58, 22–32.

Ratcliffe, J. H. and M. J. McCullagh. (1999). "Hotbeds of crime and the search for spatial accuracy." *Journal of Geographical Systems* 1, 385–98.

Rey, S. J., E. A. Mack, and J. Koschinsky. (2012). "Exploratory space-time analysis of burglary patterns." *Journal of Quantitative Criminology* 28, 509–31.

Richardson, S., A. Thomson, N. Best, and P. Elliott. (2004). "Interpreting posterior relative risk estimates in disease-mapping studies." *Environmental Health Perspectives* 112(9), 1016–25.

Richardson, S., J. J. Abellan, and N. Best. (2006). "Bayesian spatio-temporal analysis of joint patterns of male and female cancer risks in Yorkshire (UK)." *Statistical Methods in Medical Research* 15, 385–407.

Robertson, C., T. A. Nelson, Y. C. MacNab, and A. B. Lawson. (2010). "Review of methods for space-time disease surveillance." *Spatial and Spatio-Temporal Epidemiology* 1, 105–16.

Sampson, R. J. and W. B. Groves. (1989). "Community structure and crime: Testing social disorganization theory." *American Journal of Sociology* 94(4), 774–802.

Sampson, R. J., S. W. Raudenbush, and F. Earls. (1997). "Neighborhoods and violent crime: A multilevel study of collective efficacy." *Science* 288(15), 918–24.

Sampson, R.J. and S. Raudenbush. (1999). "Systematic social observation of public spaces: A new look at disorder in urban neighborhoods." *American Journal of Sociology* 105(3), 603–51.

Sampson, R. J. and S. W. Raudenbush. (2004). "Seeing disorder: Neighborhood stigma and the social construction of 'broken windows'." *Social Psychology Quarterly* 67(4), 319–42.

Shiode, S. and N. Shiode. (2014). "Microscale predictions of near-future crime concentrations with street-level geosurveillance." *Geographical Analysis* 46: 435–55.

Skogan, W. G. (1990). *Disorder and decline: Crime and the spiral of decay in American neighborhoods*. New York: The Free Press.

Spiegelhalter, D. J., N. G. Best, B. P. Carlin, and A. van der Linde. (2002). "Bayesian measures of model complexity and fit." *Journal of the Royal Statistical Society, Series B: Statistical Methodology* 64(4), 583–639.

Stern, H. S. and N. Cressie. (2000). "Posterior predictive model checks for disease mapping models." *Statistics in Medicine* 19, 2377–97.

Sturgis, P., I. Brunton-Smith, J. Kuha, and J. Jackson. (2014). "Ethnic diversity, segregation, and the social cohesion of neighbourhoods in London." *Ethnic and Racial Studies* 37(8), 1286–1309.

Taylor, R. B. (2001). *Breaking away from broken windows: Baltimore neighborhoods and the nationwide fight against crime, grime, fear, and decline*. Boulder, Colorado: Westview Press.

Thomas, A., N. Best, D. Lunn, R. Arnold, and D. Spiegelhalter. (2004). "GeoBUGS User Manual." Retrieved 20 July 2017: http://www.mrc-bsu.cam.ac.uk/wp-content/uploads/geobugs12manual.pdf.

Tiefelsdorf, M. and D. A. Griffith. (2007). "Semiparametric filtering of spatial autocorrelation: The eigenvector approach." *Environment and Planning A* 39, 1193–221.

Tzala, E. and N. Best. (2008). "Bayesian latent variable modeling of multivariate spatio-temporal variation in cancer mortality." *Statistical Methods in Medical Research* 17(1), 97–118.

Vehtari, A., A. Gelman, and J. Gabry. (2017). "Practical Bayesian model evaluation using leave-one-out cross-validation and WAIC." *Statistics and Computing* 27(5), 1413–32.

Waller, L. A., B. P. Carlin, H. Xia, and A. E. Gelfand. (1997). "Hierarchical spatio-temporal mapping of disease rates." *Journal of the American Statistical Association* 92(438), 607–17.

Weisburd, D., L. Maher, L. Sherman, M. Buerger, E. Cohn, and A. Petrisino. (1993). "Contrasting crime general and crime specific theory: The case of hot spots of crime." In *New Directions in Criminological Theory: Advances in Criminological Theory*, 45–63, edited by F. Adler and W. S. Laufer. New Brunswick, New Jersey: Transaction Publishers.

Williams, D., J. Haworth, M. Blangiardo, and T. Cheng. (2018). "A spatiotemporal Bayesian hierarchical approach to investigating patterns of confidence in the police at the neighborhood level." *Geographical Analysis*, DOI: 10.1111/gean.12160.

Xu, Y., M. L. Fiedler, and K. H. Flaming. (2005). "Discovering the impact of community policing: the broken windows thesis, collective efficacy, and citizens' judgement." *Journal of Research in Crime and Delinquency* 42(20), 147–86.

Yang, S. (2010). "Assessing the spatial-temporal relationship between disorder and violence." *Journal of Quantitative Criminology* 26, 139–63.